

Softening of the stiffness of bottlebrush polymers by mutual interaction

S. Bolisetty^a, C. Airaud^a, Y. Xu^b, A. H. E. Müller^b, L. Harnau^c, S. Rosenfeldt^a, P. Lindner^d, and M. Ballauff^{a,*}

^a*Physikalische Chemie I, University of Bayreuth, D-95440 Bayreuth, Germany*

^b*Makromolekulare Chemie II, University of Bayreuth, D-95440 Bayreuth, Germany*

^c*Max-Planck-Institut für Metallforschung, Heisenbergstr. 3, D-70569 Stuttgart, Germany,
and Institut für Theoretische und Angewandte Physik,*

Universität Stuttgart, Pfaffenwaldring 57, D-70569 Stuttgart, Germany

^d*Institut Laue-Langevin, B. P. 156X, 38042 Grenoble CEDEX 9, France*

(Dated: October 29, 2018)

We study bottlebrush macromolecules in a good solvent by small-angle neutron scattering (SANS), static light scattering (SLS), and dynamic light scattering (DLS). These polymers consist of a linear backbone to which long side chains are chemically grafted. The backbone contains about 1600 monomer units (weight average) and every second monomer unit carries side-chains with ca. 60 monomer units. The SLS- and SANS data extrapolated to infinite dilution lead to the form factor of the polymer that can be described in terms of a worm-like chain with a contour length of 380 nm and a persistence length of 17.5 nm. An analysis of the DLS data confirm these model parameters. The scattering intensities taken at finite concentration can be modeled using the polymer reference interaction site model. It reveals a softening of the bottlebrush polymers caused by their mutual interaction. We demonstrate that the persistence decreases from 17.5 nm down to 5 nm upon increasing the concentration from dilute solution to the highest concentration (40.59 g/l) under consideration. The observed softening of the chains is comparable to the theoretically predicted decrease of the electrostatic persistence length of linear polyelectrolyte chains at finite concentrations.

PACS numbers: 61.12.-q, 61.25.Hq, 61.41.+e

If polymeric side chains are grafted to a flexible or rigid polymer backbone, a cylindrical bottlebrush polymer results [1, 2, 3, 4, 5, 6, 7]. The main feature of these polymers is a marked stiffening of the main chains (see, e.g., the discussion in Refs. [5, 6, 7]). It has been demonstrated theoretically and by computer simulations that this stiffening is due to a balance of the repulsive forces originating from a steric overcrowding of the side chains and the entropic restoring force of the main chain [8]. The analysis of bottlebrush polymers by small-angle neutron scattering (SANS), small-angle X-ray scattering (SAXS) and static light scattering (SLS) in dilute solution has supported this picture by showing that these macromolecules exhibit a worm-like conformation [5, 6, 7]. However, up to now most studies on bottlebrush polymers in solution have focused on the dilute regime and *conformational ideality* has been assumed. That is, the intramolecular pair correlations are presumed to be independent of polymer concentration and can be computed based on a chain model that only accounts for intramolecular interactions between monomers. However, this assumption can fail upon increasing the polymer concentration because the polymers begin to interpenetrate leading to a medium-induced interaction between two monomers of individual polymers. As a result the persistence length is expected to decrease with increasing polymer concentration in the semidilute solution regime. Such concentration-dependent conformational changes of chain molecules have been investigated

theoretically for semidilute solutions of bottlebrush polymers [9], dense polymer solutions and melts (see, e.g., [10, 11, 12, 13, 14]), and semiflexible chain polyelectrolyte solutions (see, e.g., [15, 16, 17, 18, 19, 20, 21]). Here we present the first systematic experimental and theoretical study of concentration-dependent conformational changes of bottlebrush polymers which elucidates the importance of the medium-induced interaction on soft materials such as polymers. We demonstrate that mutual interaction between the bottlebrush polymers leads to a significant reduction of their stiffness in solution.

Figure 1 displays the repeating unit of the polymer under consideration. This polymer has been synthesized by a "grafting from" method and composed of poly(2-hydroxyethylmethacrylate) backbone grafted with poly(*t*-butyl acrylate) chains. Details of the synthesis and the characterization have been reported in Ref. [22]. SANS measurements of dilute solutions of the bottlebrush polymer in deuterated tetrahydrofuran (THF) were performed at the beamline D11 of the Institut Laue-Langevin in Grenoble, France. The incoherent contribution to the measured intensities has been determined at the highest scattering angles and subtracted in order to obtain the coherent part. In all cases absolute intensities have been obtained. Details of the data evaluation may be found in Ref. [23, 24].

Without loss of generality, the measured scattering intensity, $I(q, \phi)$, as a function of the magnitude of the scattering vector $q = |\vec{q}|$ and the volume fraction of the solute ϕ can be rendered as the product of a form factor $P(q)$ and a structure factor $S(q, \phi)$ according to

*E-mail: Matthias.Ballauff@uni-bayreuth.de; harnau@fluids.mpi-stuttgart.mpg.de

$$I(q, \phi) = \phi(\Delta\rho)^2 V_p P(q) S(q, \phi), \quad (1)$$

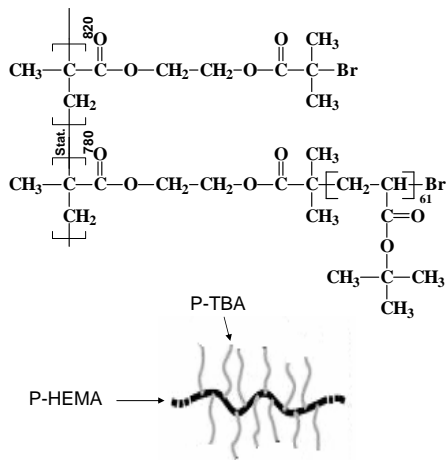


FIG. 1: Chemical structure of the investigated bottlebrush polymer consisting of a poly(2-hydroxyethylmethacrylate) (P-HEMA) backbone and poly(*t*-butyl acrylate) (p-TBA) side chains. The repeating units carrying the side chains alternate statistically with unsubstituted repeating units. The average number of repeating units per side chain is 61.

where V_p is the volume of the solute per particle and $\Delta\rho = \bar{\rho} - \rho_m$ is the contrast of the solute resulting from the difference of the average scattering length density $\bar{\rho}$ and the scattering length density ρ_m of the solvent (see Refs. [23, 24] and further citations given there). From these definitions the volume fraction ϕ follows as $\phi = c\bar{v}$ where c is the weight concentration of the dissolved polymer and \bar{v} its specific volume in the respective solvent. The latter quantity can be obtained precisely from density measurements of dilute solutions ($\bar{v} = 1.10 \pm 0.02 \text{ cm}^3/\text{g}$). These data also serve for the calculation of $\Delta\rho = -5.67 \times 10^{10} \text{ cm}^{-2}$. Figure 2 displays SANS data obtained for various concentrations of the bottlebrush polymer dissolved in deuterated tetrahydrofuran. Additional investigations were done by static light scattering in order to explore the region of smaller q -values. These data have been used to obtain the molecular weight of the bottlebrush polymer.

For sufficiently small volume fractions ϕ , the structure factor $S(q, \phi)$ can be expanded according to [24]

$$1/S(q, \phi) = 1 + 2B_{app}\phi + O(\phi^2), \quad (2)$$

where B_{app} is the apparent second virial coefficient. Hence, Eq. (2) suggests to plot $\phi/I(q, \phi)$ vs. ϕ for all q -values under consideration. The inset of Fig. 2 displays such a plot using the concentration c instead of the volume fraction ϕ . Straight lines are obtained allowing us to extrapolate the measured intensity to vanishing concentration. The open squares in Fig. 2 show the data obtained from this extrapolation together with the form factor obtained from the Pedersen-Schurtenberger model 3 [25] which includes the effect of excluded volume (see also the discussion of this problem in Ref. [7]). The scattering intensity extrapolated to vanishing concentration is well-described by the model of the worm-

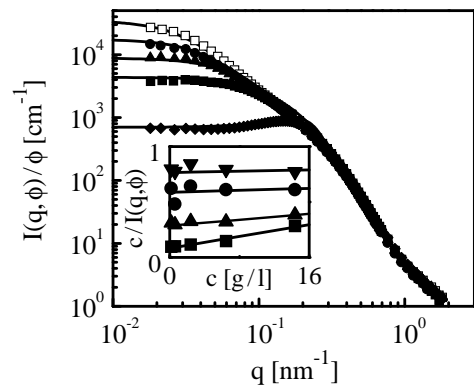


FIG. 2: Absolute scattering intensities $I(q, \phi)$ of bottlebrush polymer solutions normalized to their volume fraction ϕ . The open squares and the upper line represent the intensity extrapolated to vanishing concentration and the calculated form factor of a worm-like chain, respectively. The solid symbols denote the measured intensities for four bottlebrush polymer concentrations (circles, $c = 2.40 \text{ g/l}$; triangles, $c = 6.45 \text{ g/l}$; squares, $c = 14.35 \text{ g/l}$; diamonds, $c = 40.59 \text{ g/l}$). The four lower lines represent the corresponding intensities as obtained from the PRISM integral equation theory [Eqs. (3) and (4)] and taking into account the softening of the bottlebrush polymers (see Figs. 3 (a) and (b)). The inset shows the extrapolation of the measured intensities to vanishing concentration according to Eqs. (1) and (2) for four scattering vectors: down triangles, $q = 0.15 \text{ nm}^{-1}$; circles, $q = 0.12 \text{ nm}^{-1}$; up triangles, $q = 0.08 \text{ nm}^{-1}$; squares, $q = 0.04 \text{ nm}^{-1}$.

like chain. We obtain the contour length $L = 380 \text{ nm}$ and the persistence length $l_p = 17.5 \text{ nm}$. The radius of cross section of the chains follows as 5 nm . Static light scattering leads to a weight-average molecular weight of $7.41 \times 10^6 \text{ g/Mol}$. Together with the weight-average degree of polymerization determined from the precursor polymer a molecular weight $M_0 = 4600 \text{ g/Mol}$ of the repeating unit results. Assuming a length of the repeating unit of 0.25 nm this would lead to a mass per unit length M_L of 18.400 g/Mol/nm . Estimates of M_L using the Holtzer plot (see, e.g., Ref. [7] and further literature given there) lead to a value of ca. 19.000 g/Mol/nm . Hence, the length of the repeating unit is ca. 0.24 nm which is slightly smaller than the calculated value of 0.25 nm . A similar finding was reported recently by Zhang and coworkers [7]. Moreover, we have determined the contribution to the scattering intensity due to thermal fluctuations of the side chains.

We now turn our attention to the analysis of the scattering intensities taken at finite concentration. The form factor $P(q)$ determined by extrapolating $I(q, \phi)$ to vanishing concentration is used to calculate $S(q, \phi)$ according to Eq. (1). Fig. 3 (a) displays the experimental data obtained for four different concentrations. A quantitative understanding of correlations and interactions between various colloidal and polymeric species can be achieved using the well-established techniques of liquid-state theory. The polymer reference interaction

site model (PRISM) integral equation theory has been successfully applied to various systems, such as rodlike viruses [26], plate-like colloids [27] and dendrimers [23], flexible polymers [28], and mixtures of spherical colloids and semiflexible polymers [29]. Within the PRISM theory the structure factor $S(q, \phi)$ reads

$$S(q, \phi) = 1 + \phi h(q, \phi) / (V_p P(q, \phi)), \quad (3)$$

where $P(q, \phi)$ is the Fourier transform of the sum of the intramolecular two-point correlation functions for a given volume fraction ϕ . In the limit $\phi \rightarrow 0$ this function reduces to the form factor $P(q) \equiv P(q, \phi \rightarrow 0)$. The total correlation function $h(q, \phi)$ describes correlations between different bottlebrush polymers, and is given by the generalized Ornstein-Zernike equation

$$h(q, \phi) = P^2(q, \phi) c(q, \phi) / (1 - \phi c(q, \phi) P(q, \phi) / V_p), \quad (4)$$

where $c(q, \phi)$ is the direct correlation function. This equation is solved numerically together with the Percus-Yevick closure taking steric interactions into account [27].

In Fig. 3 (a) the experimental structure factor $S(q, \phi)$ is compared to the results of the integral equation theory for the PRISM. We have used the form factor $P(q)$ (see the upper curve in Fig. 2) as input into the generalized Ornstein-Zernike equation, i.e., $P(q, \phi) = P(q)$ in Eqs. (3) and (4). With increasing bottlebrush polymer concentration the integral equation results (dashed lines) and the experimental data (symbols) deviate. The comparison of the calculated structure factors with the experimental data demonstrates that the *concentration-independent* persistence length $l_p = 17.5$ nm and the form factor $P(q)$ may be used as input into the generalized Ornstein-Zernike equation only for very low concentrations ($c \lesssim 2.5$ g/l). For higher concentrations marked deviations are found indicating that this approach is no longer valid.

An alternative way of modeling these data is to consider a *concentration-dependent* persistence length of bottlebrush polymers and hence a concentration-dependent intramolecular correlation function $P(q, \phi)$ as input into Eqs. (3) and (4). The results for the structure factors as obtained from the PRISM integral equation theory and using concentration-dependent persistence lengths are in agreement with the experimental data both for $S(q, \phi)$ (solid lines in Fig. 3 (a)) and $I(q, \phi)$ (four lower solid lines in Fig. 2). The dependence of the persistence length on concentration shown in Fig. 3 (b) is reminiscent of the behavior of the predicted persistence length of polyelectrolytes (see Fig. 3 in Ref. [15] and Fig. 4 in Ref. [20]). Although the bottlebrush polymer solutions under consideration and the theoretically investigated polyelectrolyte solutions distinctly differ from each other, there is a significant overlap between them, namely the change of the shape of the polymers upon varying the concentration. Moreover, Fig. 3 (b) demonstrates that the concentration dependence of the calculated radii of gyration [30]

$$r_g = \sqrt{Ll_p/3 - l_p^2 + 2l_p^3/L - 2(1 - e^{-L/l_p})l_p^4/L^2} \quad (5)$$

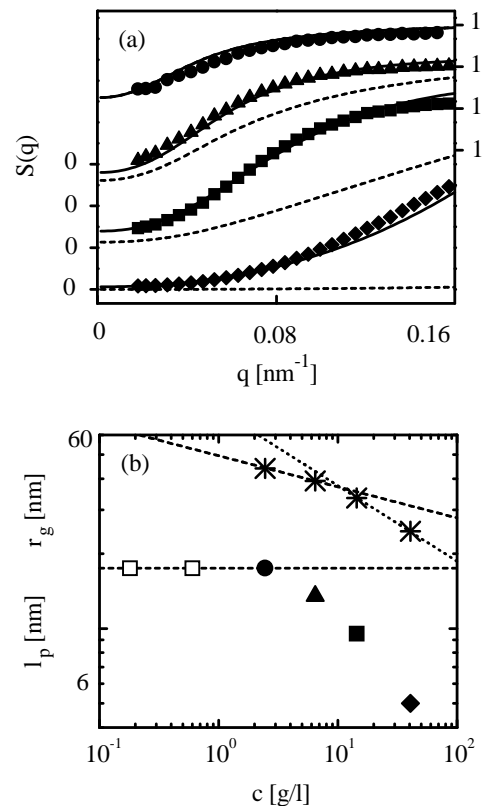


FIG. 3: (a) The structure factor $S(q, \phi)$ determined experimentally according to Eq. (1) for four concentrations (with the same symbol code as in Fig. 2). The dashed lines represent the structure factors as obtained from the PRISM integral equation theory [Eqs. (3) and (4)] and assuming a *concentration-independent* shape of the bottlebrush polymers. The solid lines represent the structure factors as obtained from the PRISM integral equation theory and using the *concentration-dependent* persistence lengths shown in (b) with the same symbol code (solid circle, triangle, square, and diamond). For reasons of clarity, the upper three data sets in (a) have been shifted up. For $c = 2.40$ g/l the dashed and solid curve coincide because the same persistence is used for both curves. The open squares in (b) denote two low concentrations which have been used for the extrapolation to infinite dilution as mentioned above. The radii of gyration as obtained from Eq. (5) are indicated in (b) by the stars. The upper dashed and dotted lines of slopes $c^{-1/8}$ and $c^{-17/56}$, respectively, represent two asymptotic scaling regimes [9].

is in agreement with scaling considerations.

In addition to static properties we have investigated dynamic properties of the bottlebrush polymers using DLS. The measured time-dependent scattering intensity is a single exponential function of time for concentrations $c \lesssim 2.5$ g/l signaling pure translational diffusion of the polymers. No contributions of internal modes such a rotation, bending, or stretching to the dynamics have been found. We have determined the hydrodynamic radius $R_h = 39 \pm 2$ nm from the measured translational diffusion coefficient. In order to understand the dynamic proper-

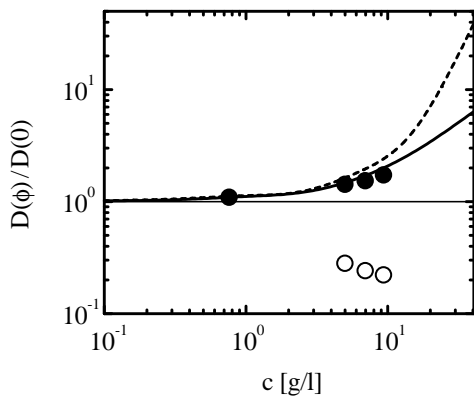


FIG. 4: Normalized cooperative diffusion coefficients $D(\phi)$ (solid circles) together with theoretical calculations using a concentration-independent [dependent] shape of the bottlebrush polymers (dashed line) [(solid line)]. The open circles denote the measured diffusion coefficients of an additional slow diffusive process for concentrations $c \gtrsim 5$ g/l.

ties of the bottlebrush polymers at low concentrations it is instructive to compare the measured hydrodynamic radius with the results for a semiflexible chain model which has been used to interpret quasi-elastic neutron and dynamic light scattering measurements on various natural and synthetic macromolecules [30] and worm-like micelles [31]. The numerical evaluation yields $R_h = 38.5$ nm which is comparable with the experimentally determined value. Moreover, we have calculated the dynamic form factor and we have found that internal modes do

not contribute to the dynamic form factor for the scattering vectors used in the light scattering experiments. However, internal modes do contribute for stiffer polymers confirming our findings concerning the stiffness of the bottlebrush polymers.

Figure 4 demonstrates that the measured cooperative diffusion coefficient $D(\phi)$ (solid circles) increases upon increasing the bottlebrush polymer concentration due to an increasing restoring force for concentration fluctuations. We have solved the equation $dI(q, \phi, t)/dt = -\Omega(q, \phi)I(q, \phi, t)$ for the time-dependent scattering intensity $I(q, \phi, t)$, where the decay rate $\Omega(q, \phi)$ depends on the solvent of the viscosity and the static scattering intensity $I(q, \phi)$ (see Ref. [28] for further details). As before in the case of the static correlation functions we have found that the cooperative diffusion coefficients $D(\phi) = \lim_{q \rightarrow 0} \Omega(q, \phi)/q^2$ as obtained from the equation for the time-dependent scattering intensity and using concentration-dependent persistence lengths (solid line in Fig. 4) are in better agreement with the experimental data than the corresponding ones using the concentration-independent persistence length $l_p = 17.5$ nm (dashed line in Fig. 4). In addition we have observed experimentally a slow diffusive process at higher concentrations (open circles in Fig. 4) which might be associated with long-range concentration fluctuations.

Acknowledgments

We wish to acknowledge financial support by the Deutsche Forschungsgemeinschaft, SFB 481, Bayreuth.

-
- [1] M. Wintermantel *et al.*, *Macromol. Chem. Rapid Comm.* **15**, 279 (1994).
 [2] M. Wintermantel *et al.*, *Angew. Chem. Int. Ed. Engl.* **34**, 1472 (1995).
 [3] M. Gerle *et al.*, *Macromolecules* **32**, 2629 (1999).
 [4] M. Zhang and A. H. E. Müller, *J. Polym. Sci.: Polym. Chem.* **43**, 3461 (2005).
 [5] S. Rathgeber *et al.*, *J. Chem. Phys.* **122**, 12904 (2005), and further references therein.
 [6] S. Rathgeber *et al.*, *Polymer* **47**, 7318 (2006).
 [7] B. Zhang, F. Gröhn *et al.*, *Macromolecules* **39**, 8440 (2006).
 [8] S. Elli *et al.*, *J. Chem. Phys.* **120**, 6257 (2004).
 [9] O. V. Borisov, T. M. Birshtein, nad Y. B. Zhulina, *Polym. Sci. U.S.S.R.* **29**, 1413 (1987).
 [10] K. S. Schweizer *et al.*, *J. Chem. Phys.* **96**, 3211 (1992).
 [11] A. Yethiraj and K. S. Schweizer, *J. Chem. Phys.* **97**, 1455 (1992).
 [12] J. Melenkevitz *et al.*, *Macromolecules* **26**, 6190 (1993).
 [13] K. S. Schweizer and J. G. Curro, *Adv. Chem. Phys.* **XCVIII**, 1 (1997).
 [14] B. J. Sung and A. Yethiraj, *J. Chem. Phys.* **122**, 234904 (2005).
 [15] M. J. Stevens and K. Kremer, *Phys. Rev. Lett.* **71**, 2228 (1993).
 [16] M. J. Stevens and K. Kremer, *J. Chem. Phys.* **103**, 1669 (1995).
 [17] A. Yethiraj, *Phys. Rev. Lett.* **78**, 3789 (1997).
 [18] A. Yethiraj, *J. Chem. Phys.* **108**, 1184 (1998).
 [19] C.-Y. Shew and A. Yethiraj, *J. Chem. Phys.* **110**, 5437 (1999).
 [20] C.-Y. Shew and A. Yethiraj, *J. Chem. Phys.* **113**, 8841 (2000).
 [21] T. Hofmann *et al.*, *J. Chem. Phys.* **118**, 6624 (2003).
 [22] M. Zhang *et al.*, *Polymer* **44**, 1449 (2003).
 [23] S. Rosenfeldt *et al.*, *ChemPhysChem* **7**, 2097 (2006).
 [24] L. Li *et al.*, *Phys. Rev.* **72**, 051504 (2005).
 [25] S. Pedersen and P. Schurtenberger, *Macromolecules* **29**, 7602, (1996).
 [26] L. Harnau and P. Reineker, *J. Chem. Phys.* **112**, 437 (2000).
 [27] L. Harnau *et al.*, *Europhys. Lett.* **53**, 729 (2001).
 [28] L. Harnau, *J. Chem. Phys.* **115**, 1943 (2001).
 [29] L. Harnau and J.-P. Hansen, *J. Chem. Phys.* **116**, 9051 (2002).
 [30] L. Harnau *et al.*, *J. Chem. Phys.* **104**, 6355 (1996); *ibid.* **109**, 5160 (1998); *Macromolecules* **30**, 6974 (1997); *ibid.* **32**, 5956 (1999).
 [31] H. von Berlepsch *et al.*, *J. Phys. Chem. B.* **102**, 7518 (1998).